

Rethinking Adversarial Inverse Reinforcement Learning: Policy Imitation, Transferable Reward Recovery and Algebraic Equilibrium Proof

Yangchun Zhang^{1,*}, Qiang Liu^{2,*}, Weiming Li^{2,*}, Yirui Zhou^{1,†}

¹Department of Mathematics, College of Sciences, Shanghai University

²School of Statistics and Management, Shanghai University of Finance and Economics
{zycstatis, zyr050798}@shu.edu.cn,
liuqiang@mail.sufe.edu.cn, li.weiming@shufe.edu.cn

Abstract

Adversarial inverse reinforcement learning (AIRL) stands as a cornerstone approach in imitation learning, yet it faces criticisms from prior studies. In this paper, we rethink AIRL and respond to these criticisms. Criticism 1 lies in Inadequate Policy Imitation. We show that substituting the built-in algorithm with soft actor-critic (SAC) during policy updating (requires multi-iterations) significantly enhances the efficiency of policy imitation. Criticism 2 lies in Limited Performance in Transferable Reward Recovery Despite SAC Integration. While we find that SAC indeed exhibits a significant improvement in policy imitation, it introduces drawbacks to transferable reward recovery. We prove that the SAC algorithm itself is not feasible to disentangle the reward function comprehensively during the AIRL training process, and propose a hybrid framework, PPO-AIRL + SAC, for a satisfactory transfer effect. Criticism 3 lies in Unsatisfactory Proof from the Perspective of Potential Equilibrium. We reanalyze it from an algebraic theory perspective.

Keywords: Adversarial inverse reinforcement learning, Policy imitation, Transferable reward recovery, Algebraic perspective

1 Introduction

Imitation learning (IL) (Pomerleau, 1991; Ng et al., 2000; Syed and Schapire, 2007; Ho and Ermon, 2016) efficiently trains a policy from expert demonstrations. Serving as a potent and practical alternative to reinforcement learning (RL) (Puterman, 2014; Sutton and Barto, 2018), it eliminates the need for designing reward signals. IL has demonstrated significant success in diverse and complex

*Equal contributions.

†Corresponding author: Yirui Zhou.

domains, such as autonomous driving (Bhattacharyya et al., 2018), robot manipulation (Jabri, 2021) and commodity search (Shi et al., 2019).

In the realm of IL, the role of inverse reinforcement learning (IRL) (Ng et al., 2000) is evident in addressing increasingly intricate sequential decision tasks. In addition, IRL effectively extracts reward functions from expert demonstrations. However, a challenge arises in IRL algorithms when distinguishing the true reward functions from those shaped by the environment dynamics (Ng et al., 1999). Thus, it can hardly produce optimal behavior in situations with varying dynamics. Addressing this limitation, Fu et al. (2018) proposed the adversarial inverse reinforcement learning (AIRL) algorithm. AIRL excels in learning disentangled rewards to maintain proper guidance through scenarios with changing dynamics. AIRL validates its efficacy by successfully mimicking the source expert behavior and recovering a robust reward function. The policy is well imitated in the source environment, and the reward function is validly recovered to re-optimize the policy by the RL algorithm in new environments.

However, AIRL often receives criticism in previous works for **inadequate policy imitation** (Criticism 1), **limited performance in transferable reward recovery** (Criticism 2) and **unsatisfactory proof from the perspective of potential equilibrium** (Criticism 3). Many IL works employ AIRL as a benchmark for comparison, claiming its shortcomings in expert imitation performance (Tucker et al., 2018; Liu et al., 2020; Ni et al., 2020; Orsini et al., 2021; Sestini et al., 2021; Xu et al., 2022; Hoshino et al., 2022) and transferable reward recovery. Even when replacing the built-in algorithm, trust region policy optimization (TRPO) (Schulman et al., 2015), with the highly sample-efficient soft actor-critic (SAC) (Haarnoja et al., 2018b) during policy optimization (known as SAC-AIRL), the transfer effect remains poor (Arnob, 2020; Xu et al., 2022; Hoshino et al., 2022). Furthermore, this inefficiency is often attributed to the inaccurate recovery of the expert’s energy, the opaque interpretations and the overly idealized decomposability condition (Liu et al., 2020; Ni et al., 2020; Cao et al., 2021; Liu et al., 2021).

In this paper, we rethink AIRL and respond to these criticisms as follows.

- For inadequate policy imitation: First, SAC’s off-policy formulation enhances sample efficiency through data reuse (Haarnoja et al., 2018a,b). Additionally, the reward given its identification with the maximum entropy (MaxEnt) Markov decision process (MDP) models (Kim et al., 2021; Cao et al., 2021) relies on leveraging SAC’s powerful training capabilities to showcase its effectiveness. Second, AIRL is vulnerable to discriminator over-fitting (Tucker et al., 2018; Sestini et al., 2021; Shi et al., 2022). To mitigate this, we implement multi-iteration policy updates following each discriminator training step, which efficiently mimics the expert. Consequently, SAC-AIRL is the recommended solution.
- For limited performance in transferable reward recovery: When AIRL shifts its focus to the transfer paradigm, it becomes crucial to completely disentangle the dynamics from the reward function, enhancing robustness in the face of varying environment dynamics. From this

standpoint, we illustrate that the SAC algorithm itself is not feasible to disentangle the reward function comprehensively during the AIRL training process, primarily because of the additional employment of the entropy term for training, as compared in theory. It also indicates the unfairness of SAC-AIRL serving as baselines in the transfer paradigm. In contrast, standard RL objective-based policy optimization methods, exemplified by the proximal policy optimization (PPO) algorithm (Schulman et al., 2017), do not encounter such issues. Therefore, PPO-AIRL (set PPO as the built-in algorithm) is recommended for obtaining a robust reward. Additionally, in new environments, the focus of the transferred reward shifts to policy training. As a result, we reintroduce the SAC algorithm for this purpose. In summary, we employ PPO-AIRL in the source environment to recover a disentangled reward and adopt the SAC algorithm to train a policy in new environments, forming the hybrid framework referred to as PPO-AIRL + SAC.

- For unsatisfactory proof from the perspective of potential equilibrium: From an algebraic theory perspective, we reanalyze that if the environment satisfies $\text{rank}(\mathbf{P} - I) = |\mathcal{S}| - 1$ (which is feasible in practical scenarios), the disentangled rewards can be extracted by AIRL. Here, \mathbf{P} is the transition matrix of the source environment, I is the identity matrix and $|\mathcal{S}|$ is the size of the finite state space. In this way, AIRL will avoid being mired in theoretical difficulties.

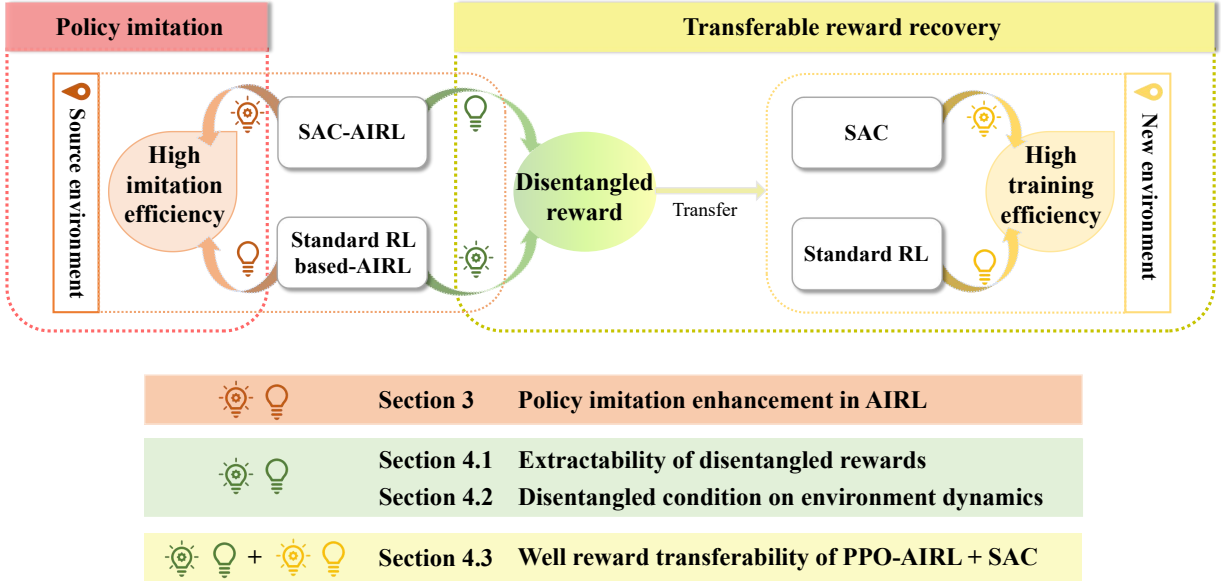


Figure 1: The overview of our analysis. Section 3 shows the strength of SAC-AIRL for policy imitation in the source environment. Section 4.1 and Section 4.2 analyze the transfer effect of the reward induced by SAC-AIRL and standard RL based-AIRL (represented by PPO-AIRL). Section 4.3 puts forward the hybrid framework PPO-AIRL + SAC for satisfactory transfer effect.

The structure of this paper is shown in Fig. 1. Code is released at <https://github.com/Garyzyr001/rethinking-airl>.

2 Background

We model the interactions between the agent and the environment through an MDP $(\mathcal{S}, \mathcal{A}, \mathcal{P}, r, \gamma, d_0)$. Particularly, \mathcal{S} and \mathcal{A} denote the finite state space and action space, respectively. $\mathcal{P} : \mathcal{S} \times \mathcal{A} \times \mathcal{S} \rightarrow [0, 1]$ represents the transition dynamics, r is the reward function, $\gamma \in (0, 1]$ is the discount factor, and $d_0 : \mathcal{S} \rightarrow [0, 1]$ denotes the initial state distribution. Stochastic policy $\pi(a|s)$ maps state $s \in \mathcal{S}$ to action $a \in \mathcal{A}$ distributions. In standard RL, the goal is to discover the optimal policy π^* that maximizes the expected return with respect to the reward function r :

$$\pi^* = \arg \max_{\pi} \mathbb{E}_{\pi} \left[\sum_t \gamma^t r(s_t, a_t) \right]. \quad (1)$$

Subsequently, we will provide preliminary background about AIRL and SAC.

2.1 Adversarial inverse reinforcement learning

IRL seeks to infer the reward function from the demonstration data \mathcal{D}^* , which is interpreted as addressing the maximum likelihood problem

$$\max_{\phi} \mathbb{E}_{\tau \sim \mathcal{D}^*} [\log p_{\phi}(\tau)],$$

where $p_{\phi}(\tau) \propto p(s_0) \prod_t p(s_{t+1}|s_t, a_t) e^{\gamma^t r_{\phi}(s_t, a_t)}$. AIRL leverages a GAN formulation to obtain solutions for this problem. To learn disentangled rewards that are invariant to changing dynamics, AIRL formalizes the discriminator as

$$D_{\phi, \Phi}(s, a, s') = \frac{\exp\{f_{\phi, \Phi}(s, a, s')\}}{\exp\{f_{\phi, \Phi}(s, a, s')\} + \pi_{\theta}(a|s)},$$

where $f_{\phi, \Phi}(s, a, s') = g_{\phi}(s, a) + \gamma h_{\Phi}(s') - h_{\Phi}(s)$, g_{ϕ} is a reward approximator, h_{Φ} is a shaping term and π_{θ} is the learned policy. Via binary logistic regression, AIRL trains $D_{\phi, \Phi}$ to classify expert data from policy samples. AIRL sets the reward as

$$r_{\phi, \Phi}(s, a, s') = \log D_{\phi, \Phi}(s, a, s') - \log(1 - D_{\phi, \Phi}(s, a, s')) \quad (2)$$

and updates the policy π_{θ} by any policy optimization method. If the ground truth reward r_{gt} only depends on the state, AIRL is able to recover the ground truth reward up to a constant, i.e., $g_{\phi}^*(s) = r_{gt}(s) + const.$

2.2 Soft actor-critic

SAC, an off-policy RL algorithm, extends Eq. (1) by incorporating an extra entropy term:

$$\pi^* = \arg \max_{\pi} \mathbb{E}_{\pi} \left[\sum_t \gamma^t (r(s_t, a_t) + \alpha \mathbb{H}(\pi(\cdot|s_t))) \right], \quad (3)$$

where α is the entropy temperature parameter. It is built upon the soft policy iteration, which alternates between soft policy evaluation and soft policy improvement (Haarnoja et al., 2018a,b). In the soft policy evaluation step, the soft Q-value is iterated by the soft Bellman equation for a fixed policy. Then the policy updates towards the exponential form of the new soft Q-function in the soft policy improvement step. With repeated application of soft policy evaluation and soft policy improvement, the soft policy iteration will converge to optimality. At this moment, the optimal soft Q-function $Q^*(s, a)$ with respect to the reward function r and the transition dynamics p satisfies

$$Q^*(s, a) = r(s, a) + \gamma \mathbb{E}_{s' \sim p, a' \sim \pi^*} [Q^*(s', a') - \alpha \log \pi^*(a'|s')]. \quad (4)$$

3 Expert behavior imitation

In this section, we investigate SAC-AIRL, and explore whether it truly benefits from the off-policy training system in SAC, the potential identifiable property by MaxEnt MDP models possessed with AIRL and multi-iteration policy updates following each discriminator training step.

In SAC-AIRL, SAC functions as the policy optimization method under the reward function specified in Eq. (2) within the context of AIRL. Moreover, for an identifiable MDP, the reward and policy must satisfy $r \cong \hat{r} \Leftrightarrow p_r = p_{\hat{r}}$, where p_r denotes the corresponding optimal trajectory distribution with respect to r (Kim et al., 2021, Definition 1). In essence, the imitated policy and reward should collectively strive for improvement towards an expert level (There is no existence of a “good” policy from a “bad” reward. We only need to promise a “good” policy, then the reward is naturally promised to be “good”). Therefore, in AIRL, a good policy optimization method (SAC) has powerful training capabilities that facilitate concurrent improvement in both reward and policy imitation. Besides, followed by (Tucker et al., 2018; Sestini et al., 2021; Shi et al., 2022), we perform multi-iterations of forward RL for each discriminator training step to deal with the discriminator over-fitting issue, ensuring a reliable training process for imitation.

Extensive evaluations demonstrate the effectiveness of SAC-AIRL (Details can be found in Appendix A).

Remark 1. *The primary aim of this section is simply to respond to the suspicions surrounding AIRL in policy imitation (Criticism 1), recognize its effectiveness, and simultaneously enhance its imitation capability to the fullest extent possible. Note that we do not claim superior performance for SAC-AIRL over advanced IL methods (Zhou et al., 2023; Swamy et al., 2023) for expert behavior imitation. In our view, the most important advantage of AIRL is placed on the recovery of transferable rewards, which is exhibited in the next section.*

4 Reward transferable analysis

In this section, we delve into the recovered reward. Initially, in Section 4.1, we examine the extractability of disentangled rewards trained by different policy optimization methods. Then Section 4.2 explores the environments capable of extracting disentangled rewards. Finally, Section 4.3 elaborates on the hybrid framework PPO-AIRL + SAC and showcases its superiority empirically.

We first recall the definition of disentangled rewards.

Definition 1 (Disentangled Rewards (Fu et al., 2018)). *A reward function $r'(s, a, s')$ is (perfectly) disentangled with respect to a ground truth reward $r_{gt}(s, a, s')$ and a set of dynamics \mathcal{P} such that under all dynamics $p \in \mathcal{P}$, the optimal policy is the same: $\pi_{r',p}^*(a|s) = \pi_{r_{gt},p}^*(a|s)$.*

Moreover, the two optimal policies (with respect to r_{gt} and r') being equal is equivalent to their corresponding Q-functions up to arbitrary state-dependent functions $f(s)$, i.e., $Q_{r',p}^*(s, a) = Q_{r_{gt},p}^*(s, a) - f(s)$.

4.1 Extractability of disentangled rewards by SAC-AIRL and PPO-AIRL

In this subsection, we explore the extractability of disentangled rewards recovered by SAC-AIRL and PPO-AIRL when the ground truth reward is state-only. We proceed with the result that SAC-AIRL fails to extract a disentangled reward during the training process.

Theorem 1. *Let $r_{gt}(s)$ be a ground truth reward, p be a dynamics model, and π_p^* be the optimal policy induced by Eq. (1) under r_{gt} and p . Suppose SAC-AIRL recovers a reward $r'(s)$ such that it produces π_p^* in p : $Q_{r',p}^*(s, a) = Q_{r_{gt},p}^*(s, a) - f(s)$. Then*

$$r'(s) = r_{gt}(s) + \gamma \mathbb{E}_{s' \sim p} [f(s')] - f(s) + \gamma \alpha \mathbb{E}_{s' \sim p, a' \sim \pi_p^*} [\log \pi_p^*(a'|s')] \quad (5)$$

holds for all $s \in \mathcal{S}$.

For detailed proof, please refer to Appendix B.

Remark 2. *We remark on the distinction between our result and (Fu et al., 2018, Theorem 5.1). (Fu et al., 2018, Theorem 5.1) is established theoretically, which utilizes the Bellman equation*

$$Q_{r',p}^*(s, a) = r'(s) + \gamma \mathbb{E}_{s' \sim p, a' \sim \pi_p^*} [Q_{r',p}^*(s', a')]$$

stemmed from the standard RL objective, as described in Eq. (1). Different from the theoretical perspective, our conclusion starts from the view of the agent during the training process. Specifically, when the framework is established on SAC (as indicated in Eq. (3)), it becomes more reasonable to consider the soft Bellman equation

$$Q_{r',p}^*(s, a) = r'(s) + \gamma \mathbb{E}_{s' \sim p, a' \sim \pi_p^*} [Q_{r',p}^*(s', a') - \alpha \log \pi_p^*(a'|s')].$$

Theorem 1 illustrates that the reward derived by SAC-AIRL is inherently connected to the imitated policy (term $\mathbb{E}_{s' \sim p, a' \sim \pi_p^*} [\log \pi_p^*(a'|s')]$ in Eq. (5)), which in turn is influenced by the source dynamics model p . In new environments with altered dynamics models, such reward poses challenges in inducing satisfactory policies. Consequently, SAC-AIRL fails to disentangle the reward from the dynamics.

Conversely, the reward recovered by PPO-AIRL satisfies

$$r'(s) = r_{gt}(s) + \gamma \mathbb{E}_{s' \sim p} [f(s')] - f(s),$$

which is immune to the dynamics model. By (Fu et al., 2018), “Under the decomposability condition, every state in the MDP can be linked with such an equality statement, meaning that $f(s)$ is constant.” Therefore, such reward equals the ground truth reward up to constants, thereby successfully disentangling from dynamics.

As a result, PPO-AIRL is able to recover a disentangled reward under a state-only ground truth reward, given that the environment satisfies certain specific conditions (e.g., the decomposability condition in (Fu et al., 2018)). In the following, we aim to delve into more precise conditions from the perspective of algebraic theory.

4.2 Disentangled condition on environment dynamics

For a state-only ground truth reward $r_{gt}(s)$ and the source transition dynamics p , let $r'(s)$ be the reward recovered by AIRL with the standard RL policy optimization method that produces an optimal policy π_p^* . Assume that for some arbitrary state-dependent function $b(s)$, $r'(s) = r_{gt}(s) + b(s)$. By (Fu et al., 2018), we have that for all s, a , $b(s) = \gamma \mathbb{E}_{s' \sim p} [f(s')] - f(s)$, i.e.,

$$b(s) = \gamma \sum_{s'} p(s'|s, a) f(s') - f(s). \quad (6)$$

Taking expectations for the optimal policy π_p^* on both sides of Eq. (6), we derive that

$$b(s) = \gamma \sum_{s'} p(s'|s) f(s') - f(s), \quad (7)$$

where $p(s'|s) = \mathbb{E}_{a \sim \pi_p^*} [p(s'|s, a)] = \sum_a \pi_p^*(a|s) p(s'|s, a)$.

Eq. (7) forms a non-homogeneous system of linear equations in terms of f . For notational simplicity, we express

$$\mathbf{P} = \begin{bmatrix} p(s^1|s^1) & \dots & p(s^{|S|}|s^1) \\ \dots & \dots & \dots \\ p(s^1|s^{|S|}) & \dots & p(s^{|S|}|s^{|S|}) \end{bmatrix}$$

be the transition matrix of the source environment. To prevent confusion with the time step specified in the subscript, here we employ superscripts to denote the state index. Let I be the identity matrix, $X = [f(s^1), \dots, f(s^{|S|})]^\top$, $b = [b(s^1), \dots, b(s^{|S|})]^\top$. Then we obtain that $(\gamma \mathbf{P} - I) X = b$.

If $\text{rank}(\gamma\mathbf{P} - I) = |\mathcal{S}| - 1$, then the homogeneous system of linear equations

$$(\gamma\mathbf{P} - I)X = 0 \tag{8}$$

has one free variable. When $\gamma \rightarrow 1$, i.e., $\text{rank}(\mathbf{P} - I) = |\mathcal{S}| - 1$, Eq. (8) has a solution that approaches $[1, \dots, 1]^\top$. At this moment, $f(s)$ is a constant, then we derive that $b(s)$ is a constant. Consequently, $r'(s)$ equals the ground truth reward $r_{gt}(s)$ up to a constant, and subsequently induces the same optimal policy.

Remark 3. *The decomposability condition in (Fu et al., 2018) transforms into $\text{rank}(\mathbf{P} - I) = |\mathcal{S}| - 1$ in our formulation. We demonstrate that under certain theoretical circumstances, there are cases that do not satisfy our rank condition but fulfill the decomposability condition, leading to an inability to achieve a constant $f(s)$ through AIRL. First, we revisit the decomposability condition.*

Definition 2 (Decomposability Condition (Fu et al., 2018)). *Two states s_1, s_2 are defined as “1-step linked” under a dynamics or transition distribution $p(s'|s, a)$ if there exists a state s that can reach s_1 and s_2 with positive probability in one time step. Also, we define that this relationship can transfer through transitivity: if s_1 and s_2 are linked, and s_2 and s_3 are linked, then we also consider s_1 and s_3 to be linked.*

If

$$\mathbf{P} = \begin{bmatrix} 1 & 0 & 0 \\ \frac{1}{3} & \frac{1}{3} & \frac{1}{3} \\ 0 & 0 & 1 \end{bmatrix},$$

such \mathbf{P} satisfies Definition 2 while $\text{rank}(\mathbf{P} - I) = 1 \neq 2 = |\mathcal{S}| - 1$. Now $f(s)$ is not a constant, which consequently results in $b(s)$ being non-constant. Under the circumstances, the environment under \mathbf{P} is incapable of extracting disentangled rewards through AIRL.

Remark 4. *Actually, $\text{rank}(\mathbf{P} - I) = |\mathcal{S}| - 1$ is untestable in real-world scenarios because the dynamics are always unknown. Fortunately, satisfying the condition is straightforward since, in theory, $\text{rank}(\mathbf{P} - I) \leq |\mathcal{S}| - 1$ naturally holds due to $\sum_j p(s^j|s^i) = 1$. Additionally, in real-world scenarios, achieving $\text{rank}(\mathbf{P} - I) = |\mathcal{S}| - 1$ is very feasible. Real-world data doesn’t demonstrate the same robust regularities as theoretical data, often making it more challenging to observe linear relationships due to factors such as complexity, diversity, noise, interference, constraints in data collection, etc.*

Here, we respond to Criticism 3 by providing a more formal and comprehensible proof from an algebraic perspective. We replace the decomposability condition with the more intuitive (rank) condition, which is highly feasible in practice. Additionally, we demonstrate that as γ approaches 1, $f(s)$ attains a constant solution, indicating a potential equilibrium. This clarifies why there may be inaccuracies in energy recovery, yet the recovered reward remains robust (Liu et al., 2021) (γ typically remains close to 1 in practice). The original proof in (Fu et al., 2018, Theorem 5.1) fails to elucidate this connection, as it lacks a direct relationship between $f(s)$ and γ .

To summarize, when the source environment satisfies $\text{rank}(\mathbf{P} - I) = |\mathcal{S}| - 1$, AIRL is capable of extracting disentangled rewards, which can then be applied for navigating policy in new environments with different dynamics.

4.3 Reward transferability verification

In this subsection, we introduce the hybrid framework PPO-AIRL + SAC. This framework utilizes PPO-AIRL to recover the reward in the source environment and then applies SAC to re-optimize the policy using this reward in the new environment (referred to as the target environment subsequently). The strengths of PPO-AIRL + SAC arise from two key aspects: (1) the effective extraction of disentangled rewards using PPO-AIRL in the source environment, and (2) the off-policy formulation with sufficient exploration capabilities of SAC in the target environment. The entire procedure of PPO-AIRL + SAC is detailed in Algorithm 1, Appendix C.

Next, we empirically assess the performance of PPO-AIRL + SAC. The experiment focuses on a 2D maze task, a quadrupedal ant agent. The 2D maze task navigates the agent (depicted in yellow) to achieve the goal (depicted in green), while the quadrupedal ant agent is trained to run forwards, which originates from Ant-v2 in OpenAI Gym (Brockman et al., 2016). These tasks are widely used platforms in IL literature (Fu et al., 2018; Qureshi et al., 2019; Ni et al., 2020). Two cases are considered in the experiment.

In Case 1, we validate the reward transfer performance when the alterations are made to the structure of the target environment. Consistent with (Fu et al., 2018), in Group 1, PointMaze-Right is set to be the source environment and PointMaze-Left is taken to be the target environment. To further assess the robustness of the learned reward, we consider two more complicated environments (PointMaze-Double & PointMaze-Multi), and add another two groups of experiments (Group 2 and Group 3). In Group 2, PointMaze-Right is set to be the source environment and PointMaze-Multi is taken to be the target environment. In Group 3, PointMaze-Double is set to be the source environment and PointMaze-Multi is taken to be the target environment. A visual display of these three groups of experiments is shown in Fig. 6(a), Appendix D.

In Case 2, we validate the reward transfer performance when the agent dynamics within the target environment are changed. Consistent with (Fu et al., 2018), in Group 4, Ant is set to be the source environment and Ant-Disabled is taken to be the target environment. Analogous to Case 1, we add another group of experiments (Group 5). In Group 5, Ant-Lengthened is taken to be the target environment, where the legs are increased twice the length of those in Ant. A graphical depiction of both groups of experiments is presented in Fig. 6(b), Appendix D.

We evaluate PPO-AIRL + SAC against three control groups: PPO-AIRL + PPO, SAC-AIRL + SAC and SAC-AIRL + PPO. Additionally, for a comprehensive comparison, off-policy inverse reinforcement learning (OPIRL) (Hoshino et al., 2022) and policy transfer by behavioral cloning (BC) (i.e., the policy imitated with BC in the source environment is directly applied to the target environment) are set as baselines to demonstrate the superiority of our results. We also incorporate

two evaluation criteria: the random policy; and the training policy induced by the SAC algorithm with the ground truth reward in the target environment, which are referred to as “Random policy” and “Oracle (SAC)”, respectively.

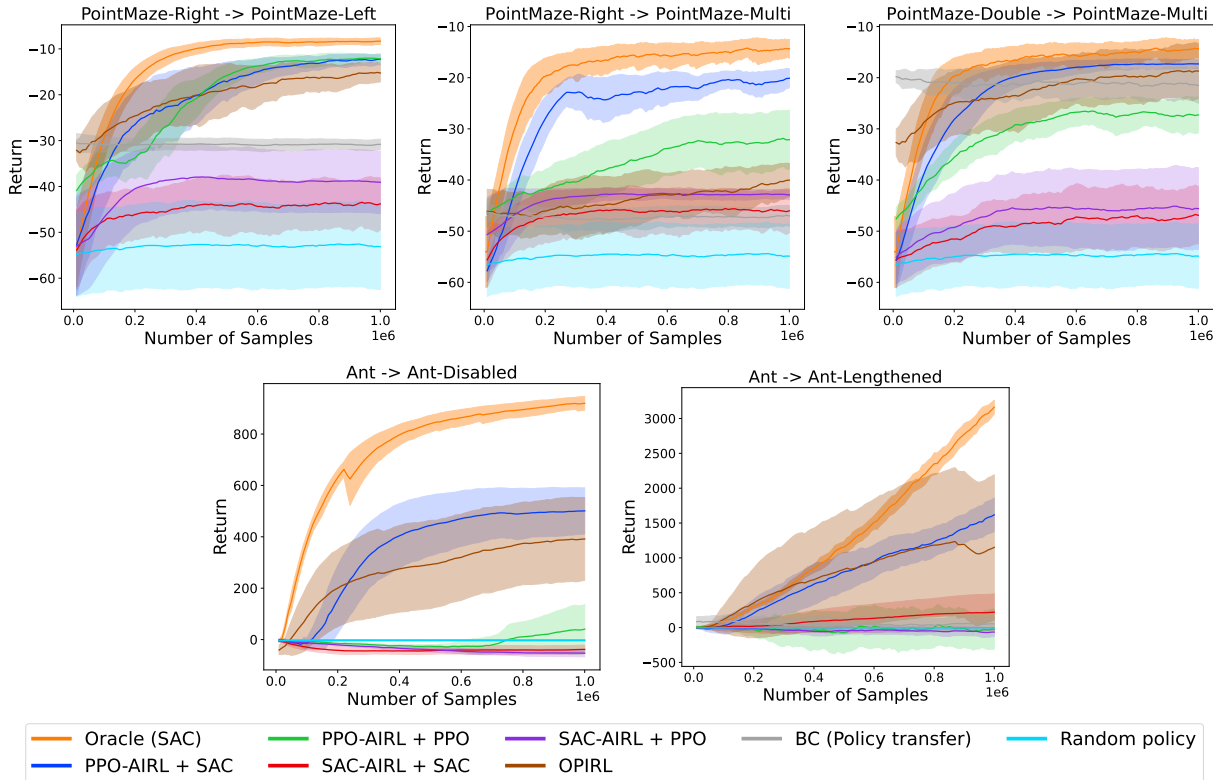


Figure 2: Transfer performance with five seeds in the target environment.

The performance of the eight algorithms is displayed in Fig. 2. We discover that PPO-AIRL + SAC and PPO-AIRL + PPO surpass other methods in Group 1. Significantly, PPO-AIRL + SAC depicts a notably superior effect in all groups, closely matching the result of the model-free algorithm. In contrast, SAC-AIRL based algorithms (SAC-AIRL + SAC and SAC-AIRL + PPO) exhibit poor performance. This observation aligns with the analysis that the reward extracted by SAC-AIRL cannot be exhaustively disentangled. Subsequently, the learned policy in the target environment benefits from the extensive exploration by SAC. In addition, it is worth noting that the performance of PPO-AIRL + SAC between Group 2 and Group 3 shows little difference (same target environment: PointMaze-Multi), which indicates the effectiveness of rewards disentangled by PPO-AIRL.

Remark 5. Here, we respond to Criticism 2 by showcasing the inadequate performance of using SAC-AIRL in the source environment or PPO (/TRPO) in the target environment, supported by both empirical evidence and theoretical analysis. On this basis, we argue that these two settings, commonly established as baselines in previous studies (Arnob, 2020; Xu et al., 2022; Hoshino et al., 2022), are not suitable. Instead, we propose a competitive framework: PPO-

AIRL + SAC.

Robustness of source reward checkpoints. Next, we validate that the transfer performance remains robust (not opportunistic) across checkpoints, maintaining consistently good performance during the training steps of the already learned reward in the source environment with our hybrid framework PPO-AIRL + SAC. The reward is identified as learned after 4×10^6 (4M) steps in PointMaze and 9M steps in Ant. It is worth noting that due to the complexity of the Ant environment (Choi and Kim, 2019), the reward function is still being learned after 4M steps and is fully learned after 9M steps.

- In PointMaze, we randomly select five checkpoints from steps 4M to 5M (steps 4.165M, 4.345M, 4.56M, 4.755M and 4.92M), together with step 5M.
- In Ant, we randomly select five checkpoints from steps 9M to 10M (steps 9.145M, 9.325M, 9.58M, 9.775M and 9.89M), together with step 10M.

The corresponding results are shown in Fig. 3. It is observed that our framework consistently demonstrates satisfactory results, which showcases the effectiveness of recovering the robust reward.

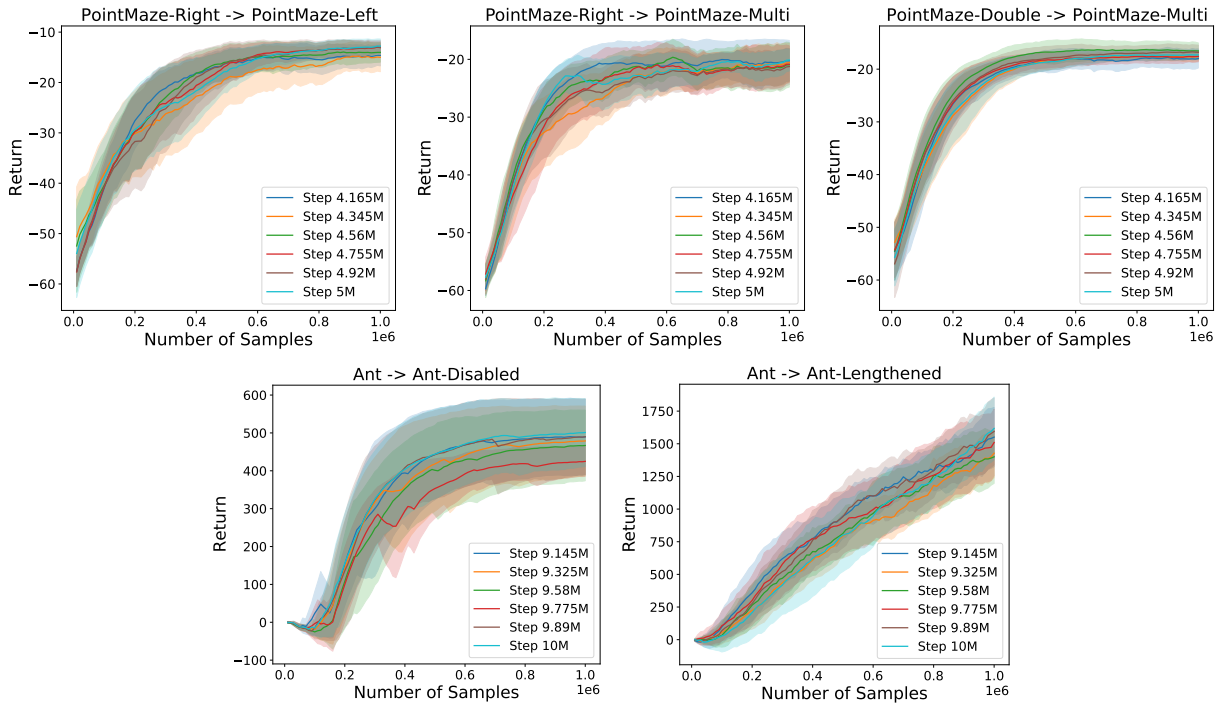


Figure 3: Performance of PPO-AIRL + SAC for different source reward checkpoints with five seeds in the target environment.

Ablation study of different source expert buffer sizes. Additionally, we conduct an ablation study on different source expert buffer sizes. The performance using expert demonstrations with buffer sizes of 10^4 and 10^6 in the source environment is deferred to Appendix E, illustrating the robustness of our hybrid framework.

5 Related work

RL (Puterman, 2014; Sutton and Barto, 2018) employs the optimization of a cumulative future reward to develop policies that effectively address sequential decision problems. Unlike RL, which often requires the manual design of a reward function, IL (Pomerleau, 1991; Ng et al., 2000; Syed and Schapire, 2007; Ho and Ermon, 2016) leverages expert demonstrations to train the agent. Within IL, IRL (Ng et al., 2000) has emerged as a significant approach. IRL, which focuses on inferring a reward function that leads to an optimal policy aligned with expert behavior, has shown remarkable effectiveness and attracted much attention in recent years (Fu et al., 2018; Kostrikov et al., 2019, 2020; Zhou et al., 2022, 2023; Freund et al., 2023). The two primary challenges in IRL are the imitation of the policy and the recovery of reward functions (Fu et al., 2018; Xu et al., 2022).

5.1 Policy imitation

IRL, by implementing distribution matching for imitation, has made substantial progress (Ho and Ermon, 2016; Kostrikov et al., 2019, 2020; Zhou et al., 2023; Freund et al., 2023). Drawing on the principles of generative adversarial networks (GANs) (Goodfellow et al., 2014) used in IL, generative adversarial imitation learning (GAIL) (Ho and Ermon, 2016) integrates a discriminator-generated reward system and a policy gradient approach to effectively mimic an expert RL policy. To address the problems of implicit bias and a large number of interactions with the environment, Kostrikov et al. (2019) designed the discriminator-actor-critic (DAC) algorithm which capitalizes on the off-policy technique to improve sample efficiency. ValueDICE (Kostrikov et al., 2020) sidesteps the methods of explicitly learning or defining rewards and directly acquires a Q-function within the distribution ratio objective. (Orsini et al., 2021) examines the two modifications (a reward shaping term and logit shift) introduced in AIRL. Subsequently, Zhou et al. (2023) conducted an in-depth analysis of various issues ranging from generalization to computation in GAIL and proposed the greedy distributional soft gradient (GDSG) algorithm by the distributional soft actor-critic (DSAC) (Ma et al., 2020; Duan et al., 2022) update for the policy. Recently, coupled flow imitation learning (CFIL) (Freund et al., 2023) effectively integrates the log ratio estimator, techniques for smoothing and regularization, the employment of flows and the use of BC (Pomerleau, 1991; Bain and Sammut, 1995) graphs, thereby yielding strong performance with a single expert trajectory. Differently, we consider employing the SAC algorithm as the policy optimization method within AIRL, and demonstrate its effectiveness in the imitation of expert behavior.

5.2 Reward recovery

One of the angles in this realm is to recover a robust reward (Fu et al., 2018; Qureshi et al., 2019; Hoshino et al., 2022; Szot et al., 2023). The AIRL algorithm (Fu et al., 2018) provides for simultaneous learning of the reward and value function, which is robust to changes in dynamics. Empowerment-regularized adversarial inverse reinforcement learning (EAIRL) (Qureshi et al., 2019)

learns empowerment by variational information maximization (Mohamed and Jimenez Rezende, 2015) to regularize the MaxEnt IRL, and subsequently obtains near-optimal rewards and policies. Their experimentation shows that the learned rewards are transferable to environments that are structurally or dynamically different from training environments. Different from GAIL and AIRL which directly process divergence minimization, Gangwani and Peng (2020) introduced another distribution as an intermediate, referred to as indirect imitation learning (I2L). I2L demonstrates its advantages in scenarios where the transition dynamics differ between the expert and imitator MDPs. Drawing upon the analytic gradient of the f -divergence between the agent’s and expert’s state distributions (regarding reward parameters), (Ni et al., 2020) devises f -IRL for retrieving a stationary reward function from the expert density via gradient descent. Based on the idea of distribution matching and AIRL, Hoshino et al. (2022) formulated OPIRL, which not only improves sample efficiency but is able to generalize to unseen environments. Further, receding-horizon inverse reinforcement learning (RHIRL) (Xu et al., 2022) shows its superiority in scalability and robustness for high-dimensional, noisy, continuous systems with black-box dynamic models. It trains a state-dependent cost function “disentangled” from system dynamics under mild conditions to be robust against noise in expert demonstrations and system control. Unlike the MaxEnt framework that aims to maximize rewards around demonstrations, behavioral cloning inverse reinforcement learning (BC-IRL) (Szot et al., 2023) optimizes the reward parameter such that its trained policy matches the expert demonstrations better. In contrast to these works, we present the disentangled condition on environment dynamics from an algebraic perspective and explore the compatibility of disentangled rewards with different policy optimization methods (SAC and the standard RL algorithm) in AIRL. Furthermore, we conduct a comprehensive analysis of the reward transfer paradigm and introduce a hybrid framework designed for a satisfactory transfer effect. This framework aims to optimize solutions in the source environment while simultaneously determining an effective training strategy in new environments.

Another interesting angle is to recover a reward of instructional significance, i.e., reward identifiability, which investigates the reward that motivates the optimal behavior to be identified up to a reasonable equivalence class (Kim et al., 2021; Cao et al., 2021; Rolland et al., 2022; Schlaginhaufen and Kamgarpour, 2023). Kim et al. (2021) formalized the reward identification problem in IRL and analyzed the relationship between identifiability and the characteristics of the MDP model. Cao et al. (2021) studied reward identification for problems with entropy regularization. They also provided the conditions for the reconstruction of time-homogeneous rewards on finite horizons and for state-only rewards. For the follow-up work, (Rolland et al., 2022) extends the results from multiple experts in IRL. (Schlaginhaufen and Kamgarpour, 2023) offers insights into reward identifiability in constrained IRL from a convex-analytic perspective.

6 Conclusion and discussion

In this paper, we respond to the three criticisms of AIRL. Regarding Criticism 1, we advocate SAC-AIRL to mimic expert behavior, which responds to (Tucker et al., 2018; Liu et al., 2020; Ni et al., 2020; Orsini et al., 2021; Sestini et al., 2021; Xu et al., 2022; Hoshino et al., 2022); Details can be found in Remark 1. Regarding Criticism 2, we advocate our hybrid framework PPO-AIRL + SAC for handling transfer learning tasks, which responds to (Arnob, 2020; Xu et al., 2022; Hoshino et al., 2022); Details can be found in Remark 5. Regarding Criticism 3, we reanalyze the argument of potential equilibrium from an algebraic theory perspective, which responds to (Liu et al., 2020; Ni et al., 2020; Cao et al., 2021; Liu et al., 2021); Details can be found in Remark 4.

The inclusion of the entropy term in SAC brings about an inability to recover the transferable reward. A straightforward strategy is to utilize the deterministic policy optimization method as the built-in algorithm in AIRL, which maintains the off-policy property and does not incorporate an entropy term (Lillicrap et al., 2016; Fujimoto et al., 2018). However, we notice the phenomenon of gradient vanishing with this strategy in policy imitation. Details for the analysis and experiment can be found in Appendix F, where we adopt twin delayed deep deterministic policy gradient (TD3) (Fujimoto et al., 2018) as an example (namely TD3-AIRL) for analysis.

Finally, the broader impact is deferred to Appendix G.

References

- Arnob, S.Y., 2020. Off-policy adversarial inverse reinforcement learning, in: 4th Lifelong Machine Learning Workshop at ICML 2020.
- Bain, M., Sammut, C., 1995. A framework for behavioural cloning. *Machine Intelligence* 15 , 103–129.
- Bhattacharyya, R.P., Phillips, D.J., Wulfe, B., Morton, J., Kuefler, A., Kochenderfer, M.J., 2018. Multi-agent imitation learning for driving simulation, in: 2018 IEEE/RSJ International Conference on Intelligent Robots and Systems (IROS), IEEE. pp. 1534–1539.
- Brockman, G., Cheung, V., Pettersson, L., Schneider, J., Schulman, J., Tang, J., Zaremba, W., 2016. OpenAI Gym. arXiv preprint arXiv:1606.01540 .
- Cao, H., Cohen, S., Szpruch, L., 2021. Identifiability in inverse reinforcement learning, in: Advances in Neural Information Processing Systems, pp. 12362–12373.
- Choi, S., Kim, J., 2019. Trajectory-based probabilistic policy gradient for learning locomotion behaviors, in: International Conference on Robotics and Automation (ICRA), IEEE. pp. 1–7.
- Duan, J., Guan, Y., Li, S.E., Ren, Y., Sun, Q., Cheng, B., 2022. Distributional soft actor-critic: Off-policy reinforcement learning for addressing value estimation errors. *IEEE Transactions on Neural Networks and Learning Systems* 33, 6584–6598.
- Freund, G.J., Sarafian, E., Kraus, S., 2023. A coupled flow approach to imitation learning, in: International Conference on Machine Learning, pp. 10357–10372.
- Fu, J., Luo, K., Levine, S., 2018. Learning robust rewards with adversarial inverse reinforcement learning, in: International Conference on Learning Representations (ICLR). Preprint retrieved from arXiv:1710.11248.
- Fujimoto, S., Hoof, H., Meger, D., 2018. Addressing function approximation error in actor-critic methods, in: International Conference on Machine Learning, pp. 1582–1591.
- Gangwani, T., Peng, J., 2020. State-only imitation with transition dynamics mismatch, in: International Conference on Learning Representations (ICLR). Preprint retrieved from arXiv:2002.11879.
- Goodfellow, I., Pouget-Abadie, J., Mirza, M., Xu, B., Warde-Farley, D., Ozair, S., Courville, A., Bengio, Y., 2014. Generative adversarial nets, in: Advances in Neural Information Processing Systems, pp. 2672—2680.
- Haarnoja, T., Zhou, A., Abbeel, P., Levine, S., 2018a. Soft actor-critic: Off-policy maximum entropy deep reinforcement learning with a stochastic actor, in: International Conference on Machine Learning, pp. 1861–1870.

- Haarnoja, T., Zhou, A., Hartikainen, K., Tucker, G., Ha, S., Tan, J., Kumar, V., Zhu, H., Gupta, A., Abbeel, P., et al., 2018b. Soft actor-critic algorithms and applications. arXiv preprint arXiv:1812.05905 .
- Ho, J., Ermon, S., 2016. Generative adversarial imitation learning, in: Advances in Neural Information Processing Systems, pp. 4565–4573.
- Hoshino, H., Ota, K., Kanazaki, A., Yokota, R., 2022. OPIRL: Sample efficient off-policy inverse reinforcement learning via distribution matching, in: International Conference on Robotics and Automation (ICRA), IEEE. pp. 448–454.
- Jabri, M.K., 2021. Robot manipulation learning using generative adversarial imitation learning, in: Proceedings of the Thirtieth International Joint Conference on Artificial Intelligence, IJCAI 2021, pp. 4893–4894.
- Kim, K., Garg, S., Shiragur, K., Ermon, S., 2021. Reward identification in inverse reinforcement learning, in: International Conference on Machine Learning, pp. 5496–5505.
- Kostrikov, I., Agrawal, K.K., Dwibedi, D., Levine, S., Tompson, J., 2019. Discriminator-actor-critic: Addressing sample inefficiency and reward bias in adversarial imitation learning, in: International Conference on Learning Representations (ICLR). Preprint retrieved from arXiv:1809.02925.
- Kostrikov, I., Nachum, O., Tompson, J., 2020. Imitation learning via off-policy distribution matching, in: International Conference on Learning Representations (ICLR). Preprint retrieved from arXiv:1912.05032.
- Lillicrap, T.P., Hunt, J.J., Pritzel, A., Heess, N., Erez, T., Tassa, Y., Silver, D., Wierstra, D., 2016. Continuous control with deep reinforcement learning, in: International Conference on Learning Representations (ICLR). Preprint retrieved from arXiv:1509.02971.
- Liu, F., Ling, Z., Mu, T., Su, H., 2020. State alignment-based imitation learning, in: International Conference on Learning Representations (ICLR). Preprint retrieved from arXiv:1911.10947.
- Liu, M., He, T., Xu, M., Zhang, W., 2021. Energy-based imitation learning, in: Proceedings of the 20th International Conference on Autonomous Agents and MultiAgent Systems, pp. 809–817.
- Ma, X., Xia, L., Zhou, Z., Yang, J., Zhao, Q., 2020. DSAC: Distributional soft actor critic for risk-sensitive reinforcement learning. arXiv preprint arXiv:2004.14547 .
- Mohamed, S., Jimenez Rezende, D., 2015. Variational information maximisation for intrinsically motivated reinforcement learning, in: Advances in Neural Information Processing Systems, pp. 2125–2133.

- Ng, A.Y., Harada, D., Russell, S., 1999. Policy invariance under reward transformations: Theory and application to reward shaping, in: International Conference on Machine Learning, pp. 278–287.
- Ng, A.Y., Russell, S.J., et al., 2000. Algorithms for inverse reinforcement learning, in: International Conference on Machine Learning, pp. 663–670.
- Ni, T., Sikchi, H., Wang, Y., Gupta, T., Lee, L., Eysenbach, B., 2020. f-irl: Inverse reinforcement learning via state marginal matching, in: Conference on Robot Learning, PMLR. pp. 529–551.
- Orsini, M., Raichuk, A., Hussenot, L., Vincent, D., Dadashi, R., Girgin, S., Geist, M., Bachem, O., Pietquin, O., Andrychowicz, M., 2021. What matters for adversarial imitation learning?, in: Advances in Neural Information Processing Systems, pp. 14656–14668.
- Pomerleau, D.A., 1991. Efficient training of artificial neural networks for autonomous navigation. *Neural Computation* 3, 88–97.
- Puterman, M.L., 2014. Markov decision processes: Discrete stochastic dynamic programming. John Wiley & Sons.
- Qureshi, A.H., Boots, B., Yip, M.C., 2019. Adversarial imitation via variational inverse reinforcement learning, in: International Conference on Learning Representations (ICLR). Preprint retrieved from arXiv:1809.06404.
- Rolland, P., Viano, L., Schürhoff, N., Nikolov, B., Cevher, V., 2022. Identifiability and generalizability from multiple experts in inverse reinforcement learning, in: Advances in Neural Information Processing Systems, pp. 550–564.
- Schlaginhaufen, A., Kamgarpour, M., 2023. Identifiability and generalizability in constrained inverse reinforcement learning, in: International Conference on Machine Learning, pp. 30224–30251.
- Schulman, J., Levine, S., Abbeel, P., Jordan, M., Moritz, P., 2015. Trust region policy optimization, in: International Conference on Machine Learning, pp. 1889–1897.
- Schulman, J., Wolski, F., Dhariwal, P., Radford, A., Klimov, O., 2017. Proximal policy optimization algorithms. arXiv preprint arXiv:1707.06347 .
- Sestini, A., Kuhnle, A., Bagdanov, A.D., 2021. Demonstration-efficient inverse reinforcement learning in procedurally generated environments, in: 2021 IEEE Conference on Games (CoG), IEEE. pp. 1–8.
- Shi, H., Li, J., Chen, S., Hwang, K.S., 2022. A behavior fusion method based on inverse reinforcement learning. *Information Sciences* 609, 429–444.

- Shi, J.C., Yu, Y., Da, Q., Chen, S.Y., Zeng, A.X., 2019. Virtual-taobao: Virtualizing real-world online retail environment for reinforcement learning, in: Proceedings of the AAAI Conference on Artificial Intelligence, pp. 4902–4909.
- Sutton, R.S., Barto, A.G., 2018. Reinforcement learning: An introduction. Cambridge, MA, USA: MIT Press.
- Swamy, G., Wu, D., Choudhury, S., Bagnell, D., Wu, S., 2023. Inverse reinforcement learning without reinforcement learning, in: International Conference on Machine Learning, pp. 33299–33318.
- Syed, U., Schapire, R.E., 2007. A game-theoretic approach to apprenticeship learning, in: Advances in Neural Information Processing Systems, pp. 1449–1456.
- Szot, A., Zhang, A., Batra, D., Kira, Z., Meier, F., 2023. BC-IRL: Learning generalizable reward functions from demonstrations, in: International Conference on Learning Representations (ICLR). Preprint retrieved from arXiv:2303.16194.
- Todorov, E., Erez, T., Tassa, Y., 2012. MuJoCo: A physics engine for model-based control, in: 2012 IEEE/RSJ International Conference on Intelligent Robots and Systems, IEEE. pp. 5026–5033.
- Tucker, A., Gleave, A., Russell, S., 2018. Inverse reinforcement learning for video games. arXiv preprint arXiv:1810.10593 .
- Xu, Y., Gao, W., Hsu, D., 2022. Receding horizon inverse reinforcement learning, in: Advances in Neural Information Processing Systems, pp. 27880–27892.
- Zhou, Y., Lu, M., Liu, X., Che, Z., Xu, Z., Tang, J., Zhang, Y., Peng, Y., Peng, Y., 2023. Distributional generative adversarial imitation learning with reproducing kernel generalization. Neural Networks 165, 43–59.
- Zhou, Y., Zhang, Y., Liu, X., Wang, W., Che, Z., Xu, Z., Tang, J., Peng, Y., 2022. Generalization and computation for policy classes of generative adversarial imitation learning, in: International Conference on Parallel Problem Solving from Nature, Springer. pp. 385–399.

A Experiments for expert behavior imitation

Empirically, we validate the effectiveness of SAC-AIRL in four common MuJoCo (Todorov et al., 2012) environments (Swimmer-v2, Hopper-v2, Walker2d-v2 and HalfCheetah-v2). The graphical display of the four environments is shown in Fig. 4. In each of these environments, we utilize a trained SAC agent as an expert to generate demonstrations. Subsequently, we collect the demonstration data with a buffer size of 10^6 and a standard deviation of 0.01.

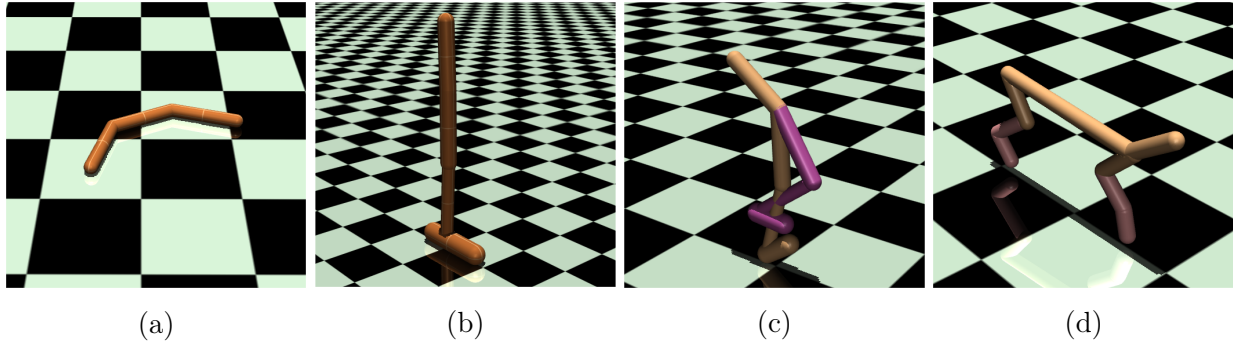


Figure 4: Expert behavior imitation environments. (a) Swimmer-v2, (b) Hopper-v2, (c) Walker2d-v2, (d) HalfCheetah-v2.

All our experiments are conducted on AMD Ryzen 9 7950X CPU and NVIDIA GeForce RTX 4090 GPU with 24G Memory. We compare SAC-AIRL (multi-iteration policy updates) against PPO-AIRL, as illustrated in Fig. 5. The solid line represents the average performance, accompanied by a shaded region that indicates the standard deviation. Additionally, the black dashed line represents the mean return of expert demonstrations. Significantly, we observe that SAC-AIRL indeed exhibits notably accelerated learning speed and superior return curve compared to PPO-AIRL, achieving near expert-level performance. This evidences the effectiveness of SAC and multi-iteration policy updates in the AIRL policy imitation process.

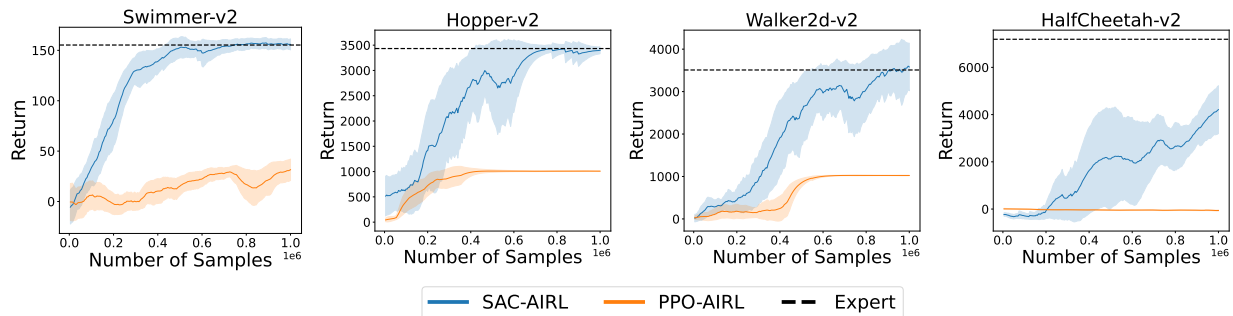


Figure 5: Performance of SAC-AIRL and PPO-AIRL with five seeds.

B Proof of Theorem 1

Proof. Note that the optimal policy π_p^* is induced by Eq. (1) under the ground truth reward r_{gt} and dynamics p . Therefore, we have that

$$Q_{r_{gt},p}^*(s, a) = r_{gt}(s) + \gamma \mathbb{E}_{s' \sim p, a' \sim \pi_p^*} [Q_{r_{gt},p}^*(s', a')].$$

$$Q_{r_{gt},p}^*(s, a) - f(s) = r_{gt}(s) + \gamma \mathbb{E}_{s' \sim p} [f(s')] - f(s) + \gamma \mathbb{E}_{s' \sim p, a' \sim \pi_p^*} [Q_{r_{gt},p}^*(s', a') - f(s')].$$

Recall the relationship between $Q_{r',p}^*(s, a)$ and $Q_{r_{gt},p}^*(s, a)$:

$$Q_{r',p}^*(s, a) = Q_{r_{gt},p}^*(s, a) - f(s).$$

Then we obtain that

$$Q_{r',p}^*(s, a) = r_{gt}(s) + \gamma \mathbb{E}_{s' \sim p} [f(s')] - f(s) + \gamma \mathbb{E}_{s' \sim p, a' \sim \pi_p^*} [Q_{r',p}^*(s', a')]. \quad (9)$$

Since SAC-AIRL recovers a reward $r'(s)$ such that it produces π_p^* in p , the optimal soft Q-function $Q_{r',p}^*(s, a)$ satisfies the form of Eq. (4), i.e.,

$$Q_{r',p}^*(s, a) = r'(s) + \gamma \mathbb{E}_{s' \sim p, a' \sim \pi_p^*} [Q_{r',p}^*(s', a') - \alpha \log \pi_p^*(a'|s')]. \quad (10)$$

Combining Eq. (9) and Eq. (10), we derive that

$$r_{gt}(s) + \gamma \mathbb{E}_{s' \sim p} [f(s')] - f(s) = r'(s) - \gamma \alpha \mathbb{E}_{s' \sim p, a' \sim \pi_p^*} [\log \pi_p^*(a'|s')].$$

Thus, we complete the proof. \square

C Entire procedure of PPO-AIRL + SAC

Algorithm 1 PPO-AIRL + SAC

- 1: **Input:** Source expert demonstrations \mathcal{D}^* .
 - 2: Initialize policy π_θ and discriminator $D_{\phi,\Phi}$ in the source environment.
 - 3: Train $D_{\phi,\Phi}$ via PPO-AIRL from \mathcal{D}^* in the source environment.
 - 4: Set reward $r_{\phi,\Phi}$ by Eq. (2).
 - 5: Train the policy with respect to $r_{\phi,\Phi}$ by SAC in the target environment.
-

D Reward transfer scenarios for reward transferability verification

The two cases of reward transfer scenarios are presented in Fig. 6 below.

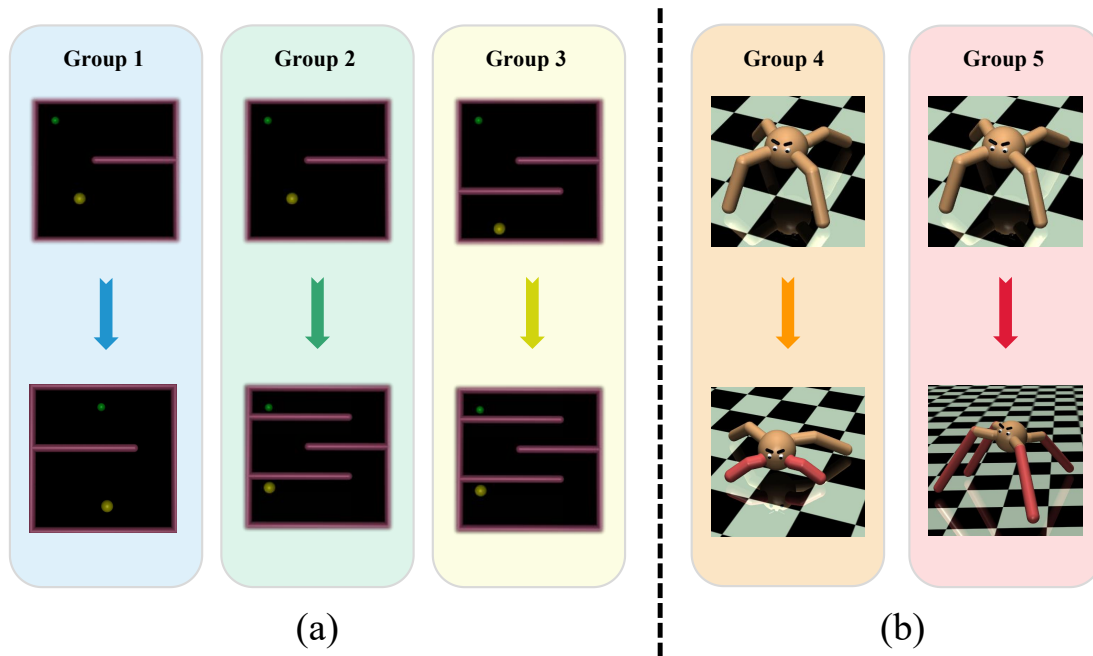


Figure 6: Two cases of reward transfer scenarios. (a) Reward transfer scenarios under changes in the environment structure (Case 1). Group 1: A reward learned in PointMaze-Right is transferred to PointMaze-Left. Group 2: A reward learned in PointMaze-Right is transferred to PointMaze-Multi. Group 3: A reward learned in PointMaze-Double is transferred to PointMaze-Multi. (b) Reward transfer scenarios under changes in the agent dynamics (Case 2). Group 4: A reward learned in Ant is transferred to Ant-Disabled. Group 5: A reward learned in Ant is transferred to Ant-Lengthened.

E Ablation experiments of different source expert buffer sizes

Here, we show the results for how varying sizes of expert demonstrations in the source environment impact our hybrid framework PPO-AIRL + SAC; see Fig. 7 as follows.

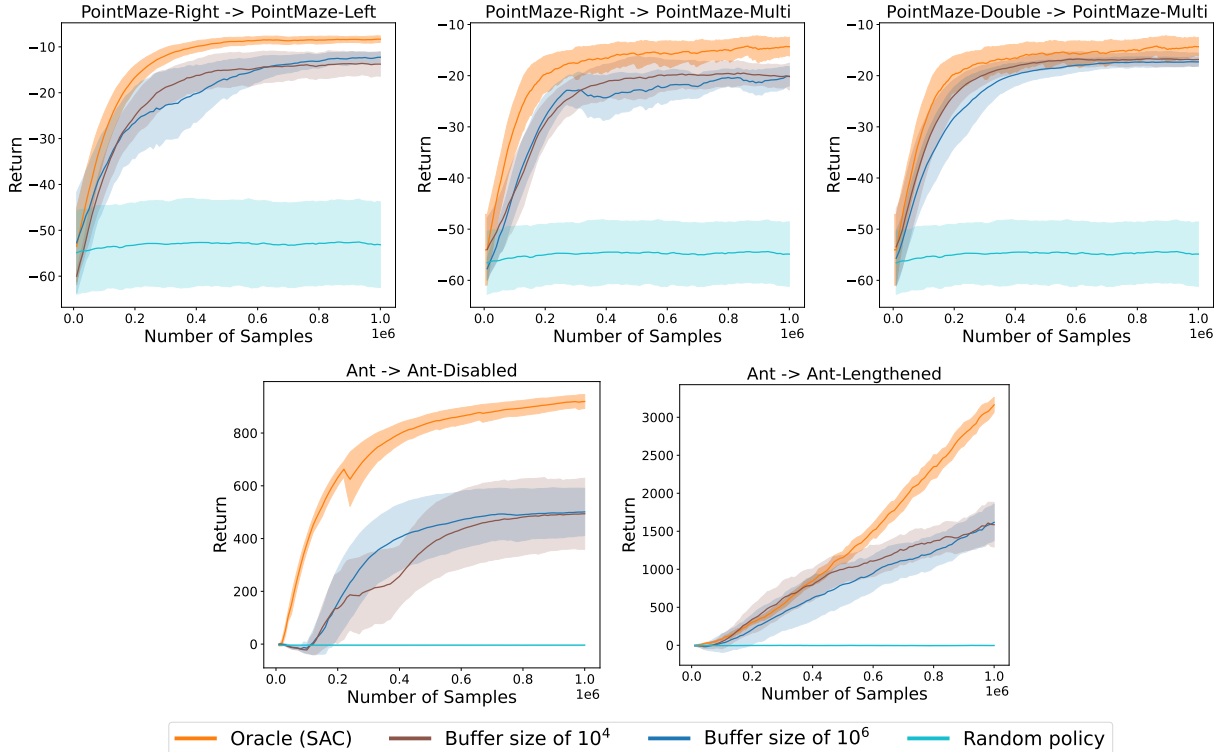


Figure 7: Performance of different source expert buffer sizes with five seeds in the target environment.

F On pathology in TD3-AIRL for expert behavior imitation

Fig. 8 exhibits the performance of TD3-AIRL for expert behavior imitation. It is observed the phenomenon of a significant variance in returns across different seeds. Such phenomenon is imputed to: The idea of GAN-based adversarial learning is distribution matching, and deterministic policies within this framework often encounter the challenge of gradient vanishing (limited overlap between the expert distribution and the initial distribution of the agent; deterministic policies lack exploration).

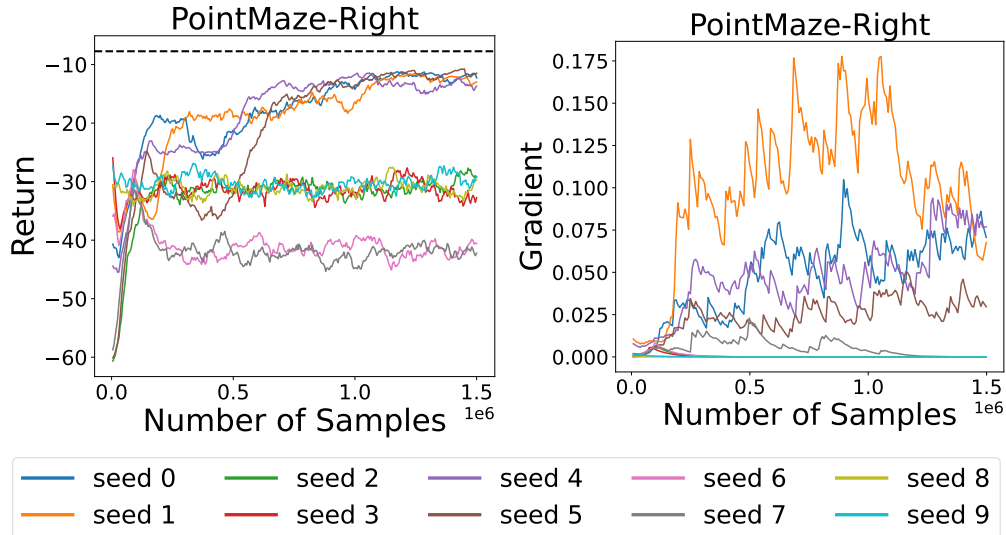


Figure 8: Performance of TD3-AIRL with 10 seeds in PointMaze-Right. **Left:** Return curves. **Right:** Absolute gradients of policy networks.

G Broader impact

We mainly focus on the framework of IL, whose main principle is to match the distribution with expert level from expert demonstrations. If the demonstrations are from non-expert (offline RL), the distribution matching mechanism of IL algorithms determines that the performance of the imitated policy tends to align with the dataset level. Consequently, IL algorithms (including our method) may fall short of achieving the desired effect in offline scenarios, which is potentially a constraint.